

# Functional clustering methods for binary longitudinal data with temporal heterogeneity

Jinwon Sohn<sup>a</sup>, Seonghyun Jeong<sup>b,c,\*</sup>, Youngmin Cho<sup>d</sup>, Taeyoung Park<sup>b,c,\*\*</sup>

<sup>a</sup>*Department of Statistics, Purdue University, IN 47907, USA*

<sup>b</sup>*Department of Applied Statistics, Yonsei University, Seoul 03722, Korea*

<sup>c</sup>*Department of Statistics and Data Science, Yonsei University, Seoul 03722, Korea*

<sup>d</sup>*Department of Computer and Information Science, University of Pennsylvania, PA 19104, USA*

---

## Abstract

In the analysis of binary longitudinal data, it is of interest to model a dynamic relationship between a response and covariates as a function of time, while also investigating similar patterns of time-dependent interactions. We present a novel generalized varying-coefficient model that accounts for within-subject variability and simultaneously clusters varying-coefficient functions, without restricting the number of clusters nor overfitting the data. In the analysis of a heterogeneous series of binary data, the model extracts population-level fixed effects, cluster-level varying effects, and subject-level random effects. Various simulation studies show the validity and utility of the proposed method to correctly specify cluster-specific varying-coefficients when the number of clusters is unknown. The proposed method is applied to a heterogeneous series of binary data in the German Socioeconomic Panel (GSOEP) study, where we identify three major clusters demonstrating the different varying effects of socioeconomic predictors as a function of age on the working status.

**Keywords:** Longitudinal data, Probit mixed models, Varying-coefficients, Partial collapsed Gibbs sampler, Dirichlet process.

---

## 1. Introduction

Mixed-effects models are commonly used in binary longitudinal studies in the social, behavioral, and health sciences. These models' popularity stems from their ability to capture longitudinal effects generated by repeated-measurement processes. To be more specific, random effects are introduced into linear models with only fixed effects to reflect the correlation between observations on the same subject. This extension also avoids some of the technical issues that can arise during the analysis of variance. For example, Stiratelli et al.

---

\*Equally contributed with the first author.

\*\*Corresponding author

*Email addresses:* [sohn24@purdue.edu](mailto:sohn24@purdue.edu) (Jinwon Sohn), [sjeong@yonsei.ac.kr](mailto:sjeong@yonsei.ac.kr) (Seonghyun Jeong), [jch0@seas.upenn.edu](mailto:jch0@seas.upenn.edu) (Youngmin Cho), [tpark@yonsei.ac.kr](mailto:tpark@yonsei.ac.kr) (Taeyoung Park)

(1984) showed that mixed-effects models have advantages over Markov models when dealing with a series of binary data because they are better at interpreting the effects of covariates and circumventing some of the difficult issues caused by unbalanced design or missing values. Other approaches to dealing with serial effects in longitudinal data provide practical recommendations by combining the mixed-effects models with other statistical methods (Varin and Czado, 2009; Guerra et al., 2012).

Adding varying coefficients has also been shown to be extremely effective for modeling of time-varying effects in longitudinal studies (Hastie and Tibshirani, 1993; Hoover et al., 1998; Wu et al., 1998; Lang and Brezger, 2004; Sun and Wu, 2005; Fan and Zhang, 2008; Lu and Zhang, 2009; Jeong and Park, 2016; Jeong et al., 2017; Park and Jeong, 2018). Such varying-coefficient functions can be easily modeled by Bayesian methods, e.g., Bayesian P-splines (Lang and Brezger, 2004), series priors (Shen and Ghosal, 2015), Gaussian process priors (Neal, 1998), and free-knot splines and adaptive knot selection (Smith and Kohn, 1996; DiMatteo et al., 2001). The main advantage of using the Bayesian approaches is that Markov chain Monte Carlo (MCMC) helps alleviate the curse of dimensionality. The method of free-knot splines and adaptive knot selection, in particular, exhibits natural local adaptation to spatially inhomogeneous smoothness, whereas other approaches require significant modifications (Smith and Kohn, 1996; Kohn et al., 2001; Ruppert et al., 2003).

Existing varying-coefficient mixed models focus on exploring common varying coefficients that are shared across all subjects, although functional linear models can estimate subject-specific varying effects through functional contrasts (Ramsey and Silverman, 2005). Because there are various sources of heterogeneity among subjects, particularly in longitudinal studies, such a common structure of varying coefficients may be oversimplified, leading to incorrect conclusions. In this regard, model-based clustering based on mixture distributions is preferable because it is easily extended to various statistical models, such as when using time series and mixed-type data to reveal latent subpopulations (Aßmann and Boysen-Hogrefe, 2011; Frühwirth-Schnatter, 2011; McParland and Gormley, 2016; Grün, 2019). One notable application of model-based clustering to mixed-effects models is clustering the subject-level coefficients rather than the responses to account for within-class heterogeneity (Lenk and DeSarbo, 2000). In addition, Aßmann and Boysen-Hogrefe (2011) applied model-based clustering to the probit mixed models to uncover latent groups in binary panel data; however, the number of clusters must be determined through cross-validation, which may be impractical in some cases due to difficult computations.

When it comes to model-based clustering, a Dirichlet process (DP) provides an effective clustering framework. A mixture model does not need to specify the exact number of mixture components in advance when using this process as a prior of mixture components because the process performs model-based clustering based on infinite mixture distributions (Kim et al., 2006; Yerebakan et al., 2014; Kyung, 2015). In particular, a stick-breaking process prior which is the approximation of the DP in a finite-dimensional space (Ishwaran and James, 2001) helps construct sampling steps for a variant of MCMC methods, and this finite process can be effectively incorporated to other statistical methodologies (Park et al., 2012, 2019). As a result, assigning the DP prior to varying coefficients in a mixed-effects model aids in revealing subpopulations within the functional coefficients without requiring an exact

number of clusters to be specified in advance.

Our contribution is threefold. First, we propose a flexible framework for simultaneously modeling population-level fixed effects, cluster-level varying effects, and subject-level random effects in the analysis of binary longitudinal data. The proposed model is a probit varying-coefficient mixed model that flexibly and adaptively identifies different subpopulations having their own varying-coefficient functions. Second, we devise new prior distributions for the efficient posterior analysis and effective functional clustering of the proposed model. In particular, it is well known that the measurement scale of data must be considered in choosing the base measure for the DP prior (Gelman et al., 2015). Because our model selection-based prior is a conditional normal prior given the model configuration, it is easier to achieve the right scale than other approaches such as the Bayesian P-spline. Third, we construct a partially collapsed Gibbs (PCG) sampler to facilitate posterior computation via the method of partial collapse (van Dyk and Park, 2008; Park and van Dyk, 2009). To maintain a transition kernel, a PCG sampler, unlike a standard Gibbs sampler, requires its steps to be performed in a specific order. We thus develop a PCG sampler that can be used in the fitting of the proposed model.

The remainder of this paper is organized as follows. In Section 2, we describe the probit varying-coefficient mixed model and discuss how the DP prior constructs model-based clustering. Section 3 specifies prior distributions and constructs efficient sampling steps based on the method of partial collapse. In Section 4, simulation studies are presented to validate the proposed method. Section 5 applies the proposed model to the GSOEP data, and Section 6 discusses the results. Appendix A contains a detailed description of the proposed method, while Appendix B describes how to install the R package for the proposed method. The R package is currently available on the first author’s github<sup>1</sup> to demonstrate that all of the results in Sections 4 and 5 can be reproduced.

## 2. Probit Varying-Coefficient Mixed Models for Functional Clustering

Let  $Y_{ij}$  represent a binary response observed at time  $t_{ij}$  for observation  $j$  on subject  $i$ , where  $i = 1, \dots, N$  and  $j = 1, \dots, n_i$ . The outcome of the response  $Y_{ij}$  can be expressed as an indicator function of the sign of a latent variable  $L_{ij}$ , i.e.,

$$Y_{ij} = I(L_{ij} > 0),$$

where the latent variable is introduced for computational convenience but can be interpreted as a utility difference between choosing  $Y_{ij} = 1$  or 0.

In longitudinal studies, a relationship between the latent variable  $L_{ij}$  and the available covariates is commonly specified by a generalized linear mixed model to account for between-subject variability. Specifically, the generalized linear mixed model is expressed as

$$L_{ij} = \mathbf{X}_i^{(j)}\boldsymbol{\beta} + \mathbf{Z}_i^{(j)}\mathbf{b}_i + \epsilon_{ij}, \quad (1)$$

---

<sup>1</sup><https://github.com/Jwsohn612/fvcc>

where  $\mathbf{X}_i = (\mathbf{x}_{i1}, \dots, \mathbf{x}_{iq})$  and  $\mathbf{Z}_i = (\mathbf{z}_{i1}, \dots, \mathbf{z}_{ir})$  are  $n_i \times q$ , and  $n_i \times r$  design matrices for subject  $i$ ,  $\mathbf{X}_i^{(j)}$  and  $\mathbf{Z}_i^{(j)}$  denote the  $j$ th row vectors of  $\mathbf{X}_i$  and  $\mathbf{Z}_i$ , respectively,  $\boldsymbol{\beta}$  is a  $q \times 1$  vector of fixed effects,  $\mathbf{b}_i$  is a  $r \times 1$  vector of random effects for subject  $i$ , and  $\epsilon_{ij}$  is an underlying error term that is assumed to follow a logistic or normal distribution in the logit or probit model, respectively. Note that the model in (1) involves multiple random effects on binary longitudinal data; for linear mixed models with multiple random effects, see Vines et al. (1996); Meng and van Dyk (1998); van Dyk (2000); Kim et al. (2013); Park and Min (2016).

In the presence of within-subject correlation over time, Jeong et al. (2017) extends the generalized linear mixed model in (1) to incorporate varying-coefficients  $\boldsymbol{\alpha}(t)$  that vary over time  $t$ , i.e.,

$$L_{ij} = \mathbf{W}_i^{(j)} \boldsymbol{\alpha}(t_{ij}) + \mathbf{X}_i^{(j)} \boldsymbol{\beta} + \mathbf{Z}_i^{(j)} \mathbf{b}_i + \epsilon_{ij}, \quad (2)$$

where  $\mathbf{W}_i = (\mathbf{w}_{i1}, \dots, \mathbf{w}_{ip})$  is  $n_i \times p$  design matrices for subject  $i$ ,  $\mathbf{W}_i^{(j)}$  denotes the  $j$ th row vector of  $\mathbf{W}_i$ ,  $\boldsymbol{\alpha}(t) = (\alpha_1(t), \dots, \alpha_p(t))^\top$  is a  $p \times 1$  vector of unknown smooth functions that vary over time  $t$ , and  $t_{ij}$  is the  $j$ th time of the  $i$ th subject. Note that  $\boldsymbol{\alpha}(t_{ij})$  is a vector of real values of  $\boldsymbol{\alpha}(t)$  evaluated at  $t_{ij}$ . The  $l$ th time-varying function in the vector  $\boldsymbol{\alpha}(t)$ , i.e.,  $\boldsymbol{\alpha}_l(t)$  can be modeled with regression splines that use a linear combination of basis functions, e.g.,

$$\mathbf{B}_l(t) = (1, t, |t - \omega_{l1}|^3, |t - \omega_{l2}|^3, \dots, |t - \omega_{lM_l}|^3)^\top, \quad (3)$$

where  $\boldsymbol{\omega}_l = (\omega_{l1}, \dots, \omega_{lM_l})$  is an ordered sequence of knot-candidate locations within the range of observed time points, for  $l = 1, \dots, p$ . The amount of smoothness for the  $l$ th regression spline is controlled by the number  $M_l$  and locations  $\boldsymbol{\omega}_l$ .

To account for heterogeneity among the subjects while borrowing strength across the different subjects, we consider allocating each subject to its own cluster with different functions of varying-coefficients. To do so, we represent the set of functions  $\boldsymbol{\alpha}(t)$  in (2) as the subject-level varying-coefficients, i.e.,  $\boldsymbol{\alpha}_i(t) = (\alpha_{i1}(t), \dots, \alpha_{ip}(t))^\top$ . Each of the unknown subject-specific varying-coefficient functions is assumed to fall in the linear span of a set of its own basis functions according to basis selection, i.e.,

$$\alpha_{il}(t) \approx (\mathbf{B}_l(t) \odot \boldsymbol{\gamma}_{il})^\top \boldsymbol{\phi}_{il},$$

where  $\odot$  denotes element-wise multiplication of vectors in accordance with values of  $\boldsymbol{\gamma}_{il}$ ,  $\boldsymbol{\gamma}_{il} = (1, \gamma_{il0}, \gamma_{il1}, \dots, \gamma_{ilM_l})^\top$  denotes an  $(M_l + 2) \times 1$  vector of indicator variables for basis inclusion,  $\gamma_{ilm} = 1$  represents that the  $(m + 2)$ th element in  $\boldsymbol{\gamma}_{il}$  is used as a basis function, and  $\boldsymbol{\phi}_{il}$  denotes an  $(M_l + 2) \times 1$  vector of basis coefficients corresponding to the  $l$ th varying-coefficient for subject  $i$ . The first element in  $\boldsymbol{\gamma}_{il}$  equals one, so the constant basis function in (3) always remains in the model. When the corresponding covariate has no interaction with time, we have  $\gamma_{ilm} = 0$  for  $m = 0, \dots, M_l$ , and the model in (2) is reduced to the generalized linear mixed model in (1). That is, when the true varying-coefficient function is constant, our model can estimate it as a constant function by choosing  $\gamma_{ilm} = 0$  for  $m = 0, \dots, M_l$ , reducing modeling bias and avoiding the possibility of overfitting. When the true varying-coefficient function is nonlinear, selecting appropriate knots allows the estimated function to

adapt to the true one's curvature. That is, we use data to adjust the spatially inhomogeneous smoothness of a varying-coefficient function, so that more knots are used in a high-curvature region and fewer knots in a low-curvature region. This implies that we do not need to a priori determine whether a varying-coefficient function is constant, linear, or nonlinear (Jeong and Park, 2016; Jeong et al., 2017, 2022). The value of  $M_l$  for the knot-candidates is not crucial as long as it is large enough to capture the global and local characteristics of a function. Following the literature (e.g., Kohn et al., 2001), we recommend using 20 to 30 knot-candidates chosen by the sample quantiles of the time variable  $t$ . If the time variable is repeatedly observed at some points in time,  $M_l$  should not be larger than the number of the non-duplicated values for  $t$ .

Next, the individualized vector of functions  $\boldsymbol{\alpha}_i(t)$  is given the DP prior, which induces functional clustering with respect to the functions. Section 3.1 describes how the model leverages the DP prior to cluster varying-coefficients in detail. Let  $C_i = k$  denote that subject  $i$  belongs to cluster  $k$  sharing identical basis functions for varying-coefficients, for  $i = 1, \dots, N$  and  $k = 1, \dots, K$ . Then through the DP prior, we have  $\boldsymbol{\alpha}_i(t) = \boldsymbol{\alpha}_k^*(t)$ , which implies  $\boldsymbol{\gamma}_{il} = \boldsymbol{\gamma}_{kl}^*$  and  $\boldsymbol{\phi}_{il} = \boldsymbol{\phi}_{kl}^*$  as well. To be specific,

$$\alpha_{il}(t) = \alpha_{kl}^*(t) \approx (\mathbf{B}_l(t) \odot \boldsymbol{\gamma}_{kl}^*)^\top \boldsymbol{\phi}_{kl}^*, \quad l = 1, \dots, p, \quad (4)$$

for the  $i$ th subject who is allocated to cluster  $k$ , having  $C_i = k$ . Thus, for the  $i$ th subject, the model in (2) can be represented in a matrix form,

$$\mathbf{L}_i = \sum_{l=1}^p (\mathbf{w}_{il} \odot \alpha_{C_il}^*(t_{ij})|_{j=1}^{n_i}) + \mathbf{X}_i \boldsymbol{\beta} + \mathbf{Z}_i \mathbf{b}_i + \boldsymbol{\epsilon}_i, \quad (5)$$

where  $\alpha_{C_il}^*(t_{ij})|_{j=1}^{n_i} = (\alpha_{C_il}^*(t_{i1}), \dots, \alpha_{C_il}^*(t_{in_i}))^\top$  is a  $n_i \times 1$  vector of real values,  $\mathbf{L}_i$  is an  $n_i \times 1$  vector of latent variables, and  $\boldsymbol{\epsilon}_i$  is a  $n_i \times 1$  error vector. This representation implies that the clustering process is implemented with information about only dynamic covariates.

To express (5) with the approximation in (4), we define an  $n_i \times (M_l + 2)$  matrix  $\mathbf{B}_{il}^* = (\oplus_{j=1}^{n_i} (\mathbf{B}_l(t_{ij}) \odot \boldsymbol{\gamma}_{C_il}^*))^\top$  where  $\oplus$  represents the direct sum of vectors or matrices, for the  $l$ th covariate of the  $i$ th subject. It is obvious that this matrix can have zero column vectors when the corresponding elements of  $\boldsymbol{\gamma}_{C_il}^*$  are zero. By removing the columns of 0's, we can obtain an  $n_i \times |\boldsymbol{\gamma}_{C_il}^*|$  submatrix of  $\mathbf{B}_{il}^*$ , which is denoted by  $\mathbf{B}_{il}^*$ , where  $|\boldsymbol{\gamma}_{C_il}^*| = \sum_m \gamma_{Cilm}^*$ . Then the model in (5) can be written as

$$\mathbf{L}_i = \mathbf{W}_{i(\boldsymbol{\gamma}_{C_i}^*)}^* \boldsymbol{\phi}_{(\boldsymbol{\gamma}_{C_i}^*)}^* + \mathbf{X}_i \boldsymbol{\beta} + \mathbf{Z}_i \mathbf{b}_i + \boldsymbol{\epsilon}_i, \quad (6)$$

where  $\boldsymbol{\phi}_{(\boldsymbol{\gamma}_{C_i}^*)}^*$  is a vector of cluster-level basis coefficients whose size is the sum of all elements of  $\boldsymbol{\gamma}_{C_i}^*$ . It is

$$\boldsymbol{\phi}_{(\boldsymbol{\gamma}_{C_i}^*)}^* = (\boldsymbol{\phi}_{\boldsymbol{\gamma}_{C_i}^{*1}}^*, \dots, \boldsymbol{\phi}_{\boldsymbol{\gamma}_{C_i}^{*p}}^*)^\top \in \mathbb{R}^{|\boldsymbol{\gamma}_{C_i}^*| \times 1},$$

where  $|\boldsymbol{\gamma}_{C_i}^*| = \sum_{l,m} \gamma_{C_i l m}^*$  and  $\boldsymbol{\phi}_{\gamma_{C_i l}^*}^*$  is a  $|\boldsymbol{\gamma}_{C_i l}^*| \times 1$  subvector of  $\boldsymbol{\phi}_{C_i l}^*$  whose elements correspond to nonzero columns of  $\mathbf{B}_{il}^*$ . Then, the design matrix  $\mathbf{W}_{i(\gamma_{C_i}^*)}^*$  is constructed by multiplying each set of selected basis terms to each column of  $\mathbf{W}_i$ , i.e.,

$$\mathbf{W}_{i(\gamma_{C_i}^*)}^* = \left[ \mathbf{w}_{i1} \mathbf{1}_{|\gamma_{C_i l}^*|}^\top \odot \mathbf{B}_{i1}^*, \dots, \mathbf{w}_{ip} \mathbf{1}_{|\gamma_{C_i p}^*|}^\top \odot \mathbf{B}_{ip}^* \right] \in \mathbb{R}^{n_i \times |\gamma_{C_i}^*|}.$$

where  $\mathbf{1}_{|\gamma_{C_i l}^*|}$  is a vector of ones in  $\mathbb{R}^{|\gamma_{C_i l}^*| \times 1}$ .

### 3. Bayesian Analysis

#### 3.1. Dirichlet Process Prior

In this paper, the Dirichlet process (DP) is used as a prior distribution to cluster  $\boldsymbol{\alpha}_i(t)$ , and this clustering procedure is equivalent to clustering the set of  $(\boldsymbol{\phi}_i, \boldsymbol{\gamma}_i)$ , where  $\boldsymbol{\phi}_i = (\boldsymbol{\phi}_{i1}, \dots, \boldsymbol{\phi}_{ip})^\top$  and  $\boldsymbol{\gamma}_i = (\boldsymbol{\gamma}_{i1}, \dots, \boldsymbol{\gamma}_{ip})^\top$ , as implied in (4). This process assigning the DP prior to the set of  $(\boldsymbol{\phi}_i, \boldsymbol{\gamma}_i)$  is expressed as

$$\begin{aligned} (\boldsymbol{\phi}_i, \boldsymbol{\gamma}_i) | \mathcal{H} &\stackrel{\text{iid}}{\sim} \mathcal{H}, \quad i = 1, \dots, N, \\ \mathcal{H} &\sim \text{DP}(\nu, \mathcal{H}_0), \end{aligned}$$

where  $\nu > 0$  and  $\mathcal{H}_0$  is a base distribution that randomly generates cluster-level parameters for  $(\boldsymbol{\phi}_i, \boldsymbol{\gamma}_i)$ . As another representation of the DP, it is worthwhile to look at the stick-breaking process (Ishwaran and James, 2001) that allows the truncation of the summation in the DP after some large  $K$  components, i.e.,

$$\mathcal{H}(\cdot) = \sum_{k=1}^{\infty} \pi_k \delta_{(\boldsymbol{\phi}_k^*, \boldsymbol{\gamma}_k^*)}(\cdot) \approx \sum_{k=1}^K \pi_k \delta_{(\boldsymbol{\phi}_k^*, \boldsymbol{\gamma}_k^*)}(\cdot), \quad (\boldsymbol{\phi}_k^*, \boldsymbol{\gamma}_k^*) \stackrel{\text{iid}}{\sim} \mathcal{H}_0, \quad (7)$$

where  $\boldsymbol{\phi}_k^* = (\boldsymbol{\phi}_{k1}^*, \dots, \boldsymbol{\phi}_{kp}^*)^\top$  and  $\boldsymbol{\gamma}_k^* = (\boldsymbol{\gamma}_{k1}^*, \dots, \boldsymbol{\gamma}_{kp}^*)^\top$  are the parameters for cluster  $k$ ,  $\delta_{(\boldsymbol{\phi}_k^*, \boldsymbol{\gamma}_k^*)}(\cdot)$  is a Dirac measure at  $(\boldsymbol{\phi}_k^*, \boldsymbol{\gamma}_k^*)$ ,  $\pi_k$  is the probability mass at atom  $(\boldsymbol{\phi}_k^*, \boldsymbol{\gamma}_k^*)$ , and  $K$  is a finite truncation for the maximum number of clusters. The equation in (7) means that the model in (6) explores latent subpopulations by limiting the maximum number of subpopulations to  $K$ , not to infinity; see (Ishwaran and James, 2001) for theoretical arguments. Meanwhile, the set of cluster-level parameters,  $\boldsymbol{\phi}_k^*$  and  $\boldsymbol{\gamma}_k^*$ , is drawn from the base distribution  $\mathcal{H}_0$ , and the random weight  $\pi_k$  derives from a set of random variables that each follows a beta distribution, i.e.,

$$\pi_k = \pi_k(\mathbf{V}) = V_k \prod_{\ell < k} (1 - V_\ell), \quad V_k \stackrel{\text{ind}}{\sim} \text{Beta}(1, \nu), \quad k = 1, \dots, K - 1,$$

where  $\mathbf{V} = \{V_1, \dots, V_K\}$  and  $V_K = 1$ , which guarantees the sum of all random weights is equal to one. Then, we can write  $P(C_i = k | \mathbf{V}) = \pi_k(\mathbf{V})$ . The specification of  $\nu$  may affect clustering performance. As  $\nu$  goes to 0, the concentration toward the existing clusters gets stronger by decreasing the probability that a vector  $(\boldsymbol{\phi}_i, \boldsymbol{\gamma}_i)$  forms a new cluster. In this work, we set  $\nu = 1$  by default so that every subject has the equal probability for shaping a new cluster (Wallach et al., 2010).

### 3.2. Prior Specification for the Submodel Parameters

This section discusses the specification of prior distributions of each model component. The set of indicator variables  $\gamma_{kl}^*$  has a beta-binomial prior distribution, i.e.,

$$p(\gamma_{kl}^*) \propto B(|\gamma_{kl}^*| + a, M_l + 1 - |\gamma_{kl}^*| + b),$$

for  $k = 1, \dots, K$  and  $l = 1, \dots, p$ , where  $B(\cdot, \cdot)$  denotes the beta function. If  $a = b = 1$ , this prior distribution allocates equal probabilities for the number of active knots (Scott and Berger, 2010). This choice has been shown work successfully for function estimation with knot selection (Jeong and Park, 2016; Jeong et al., 2017).

For the basis coefficients  $\phi_{(\gamma_k^*)}^*$  that have varying dimension in each iteration, we consider the following mixture of  $g$ -priors,

$$\begin{aligned} \phi_{(\gamma_k^*)}^* | (\gamma_k^*, \tau_k) &\stackrel{\text{ind}}{\sim} N_{|\gamma_k^*|} \left( \mathbf{0}, \tau_k \mathbf{R}_{k(\gamma_k^*)}^{-1} \right), \\ \mathbf{R}_{k(\gamma_k^*)} &= \sum_{i=1}^N \mathbf{W}_{i(\gamma_k^*)}^{\star\top} \mathbf{W}_{i(\gamma_k^*)}^*, \quad k = 1, \dots, K, \\ \tau_k &\stackrel{\text{iid}}{\sim} \text{IG}(1/2, N/2), \quad k = 1, \dots, K. \end{aligned} \quad (8)$$

By characterizing the scale parameter with the total number of subjects, the prior in (8) corresponds to a Zellner-Siow prior, which is a multivariate Cauchy prior marginally for  $\phi_{(\gamma_k^*)}^*$  (Liang et al., 2008). Therefore, the base measure  $\mathcal{H}_0$  is constructed by combining a beta-binomial distribution and a multivariate Cauchy distribution.

The prior in (8) has a few desirable properties. First, the prior distribution is invariant to linear transformations of the design matrix (Zellner, 1986). That is, the posterior distribution of the varying-coefficients is invariant to linear transformation of the basis functions in (3). More importantly, the prior (8) induces a reasonable scale for the base measure  $\mathcal{H}_0$ . It is well known that the scale of the data must be appropriately considered in choosing the base measure (Gelman et al., 2015). Our experience shows that the prior provides a suitable scale for the base measure, which may not be straightforward with other Bayesian methods for function estimation, such as the Bayesian P-spline (Lang and Brezger, 2004).

As for the fixed effects  $\beta$ , we assign a multivariate normal distribution whose covariance matrix is positive definite, i.e.,

$$\beta \sim N_q(\mathbf{0}, \mathbf{P}).$$

For practical purposes,  $\mathbf{P}$  can be chosen as a diagonal matrix with large diagonal entries. For random effects, a multivariate normal distribution is used to generate the effects,

$$\mathbf{b}_i | \Psi \stackrel{\text{iid}}{\sim} N_r(\mathbf{0}, \Psi), \quad i = 1, \dots, N,$$

where  $\Psi$  is the covariance matrix of the random effects and has an inverse-Wishart prior,

$$\Psi \sim \text{IW}(u, \mathbf{D}).$$

In our study,  $u$  and  $\mathbf{D}$  are fixed in advance to make the prior distribution diffuse.

---

**Algorithm 1:** One iteration of the Gibbs sampler

---

```

Initialize:  $(\phi_{(\gamma^*)}^*, \gamma^*, \beta, \mathbf{b}, \mathbf{C}, \mathbf{V}, \tau, \Psi, \mathbf{L})$ 
for  $k = 1, 2, \dots, K$  do
  for  $l = 1, 2, \dots, p$  do
    Step 1: Draw  $\gamma_{kl}^*$  from  $p(\gamma_{kl}^* | \gamma_{-kl}^*, \phi_{(\gamma^*)}^*, \mathbf{b}, \beta, \mathbf{C}, \mathbf{V}, \tau, \Psi, \mathbf{L}, \mathbf{Y})$ 
  for  $k = 1, 2, \dots, K$  do
    Step 2: Draw  $V_k$  from  $p(V_k | \phi_{(\gamma^*)}^*, \mathbf{b}, \gamma^*, \beta, \mathbf{C}, \tau, \Psi, \mathbf{L}, \mathbf{Y})$ 
  for  $k = 1, 2, \dots, K$  do
    Step 3: Draw  $\phi_{(\gamma_k^*)}^*$  from  $p(\phi_{(\gamma_k^*)}^* | \mathbf{b}, \gamma^*, \beta, \mathbf{C}, \mathbf{V}, \tau, \Psi, \mathbf{L}, \mathbf{Y})$ 
  for  $i = 1, 2, \dots, N$  do
    Step 4: Draw  $\mathbf{b}_i$  from  $p(\mathbf{b}_i | \phi_{(\gamma^*)}^*, \gamma^*, \beta, \mathbf{C}, \mathbf{V}, \tau, \Psi, \mathbf{L}, \mathbf{Y})$ 
  for  $k = 1, 2, \dots, K$  do
    Step 5: Draw  $\tau_k$  from  $p(\tau_k | \phi_{(\gamma^*)}^*, \gamma^*, \beta, \mathbf{b}, \mathbf{C}, \mathbf{V}, \Psi, \mathbf{L}, \mathbf{Y})$ 
  Step 6: Draw  $\Psi$  from  $p(\Psi | \phi_{(\gamma^*)}^*, \gamma^*, \beta, \mathbf{b}, \mathbf{C}, \mathbf{V}, \tau, \mathbf{L}, \mathbf{Y})$ 
  for  $i = 1, 2, \dots, N$  do
    for  $j = 1, 2, \dots, n_i$  do
      Step 7: Draw  $L_{ij}$  from  $p(L_{ij} | \phi_{(\gamma^*)}^*, \gamma^*, \beta, \mathbf{b}, \mathbf{C}, \mathbf{V}, \tau, \Psi, \mathbf{Y})$ 
  for  $i = 1, 2, \dots, N$  do
    Step 8: Draw  $C_i$  from  $p(C_i | \phi_{(\gamma^*)}^*, \gamma^*, \beta, \mathbf{b}, \mathbf{V}, \tau, \Psi, \mathbf{L}, \mathbf{Y})$ 
  Step 9: Draw  $\beta$  from  $p(\beta | \phi_{(\gamma^*)}^*, \gamma^*, \mathbf{b}, \mathbf{C}, \mathbf{V}, \tau, \Psi, \mathbf{L}, \mathbf{Y})$ 

```

---

### 3.3. Partially Collapsed Gibbs (PCG) Sampler

Given the prior distributions in Section 3.2, we propose an efficient sampling algorithm used to simulate the target posterior distribution,

$$p(\phi_{(\gamma^*)}^*, \gamma^*, \beta, \mathbf{b}, \mathbf{C}, \mathbf{V}, \tau, \Psi, \mathbf{L} | \mathbf{Y}), \quad (9)$$

where  $\gamma^* = \{\gamma_1^*, \dots, \gamma_K^*\}$ ,  $\phi_{(\gamma^*)}^* = \{\phi_{(\gamma_1^*)}^*, \dots, \phi_{(\gamma_K^*)}^*\}$ ,  $\mathbf{b} = \{\mathbf{b}_1, \dots, \mathbf{b}_N\}$ ,  $\tau = \{\tau_1, \dots, \tau_K\}$ ,  $\mathbf{C} = \{C_1, \dots, C_N\}$ ,  $\mathbf{L} = \{\mathbf{L}_1, \dots, \mathbf{L}_N\}$ , and  $\mathbf{Y} = \{\mathbf{Y}_1, \dots, \mathbf{Y}_N\}$  denoting  $\mathbf{Y}_i$  as a set of binary responses for subject  $i$ . First, we begin with the Gibbs sampler that iterates among full conditional distributions derived from (9). One iteration of the Gibbs sampler is given in Algorithm 1, which is repeated until convergence.

To improve the convergence characteristics of Algorithm 1, we devise the PCG sampler based on marginalization, permutation, and trimming tools (van Dyk and Park, 2008). Specifically, we consider marginalizing the random effects  $\mathbf{b}$  and the basis coefficients  $\phi_{(\gamma^*)}^*$  in (9), thereby producing the following marginal distributions,

$$p(\gamma^*, \beta, \mathbf{C}, \mathbf{V}, \tau, \Psi, \mathbf{L} | \mathbf{Y}), \quad (10)$$

$$p(\phi_{(\gamma^*)}^*, \gamma^*, \beta, \mathbf{C}, \mathbf{V}, \tau, \Psi, \mathbf{L} | \mathbf{Y}). \quad (11)$$

---

**Algorithm 2:** One iteration of the PCG sampler

---

```
Initialize:  $(\phi_{(\gamma^*)}^*, \gamma^*, \beta, \mathbf{b}, \mathbf{C}, \mathbf{V}, \tau, \Psi, \mathbf{L})$ 
for  $k = 1, 2, \dots, K$  do
  for  $l = 1, 2, \dots, p$  do
    Step 1: Draw  $\gamma_{kl}^*$  from  $p(\gamma_{kl}^* | \gamma_{-kl}^*, \beta, \mathbf{C}, \mathbf{V}, \tau, \Psi, \mathbf{L}, \mathbf{Y})$ 
  for  $k = 1, 2, \dots, K$  do
    Step 2: Draw  $V_k$  from  $p(V_k | \gamma^*, \beta, \mathbf{C}, \tau, \Psi, \mathbf{L}, \mathbf{Y})$ 
  for  $k = 1, 2, \dots, K$  do
    Step 3: Draw  $\phi_{(\gamma_k)}^*$  from  $p(\phi_{(\gamma_k)}^* | \gamma^*, \beta, \mathbf{C}, \mathbf{V}, \tau, \Psi, \mathbf{L}, \mathbf{Y})$ 
  for  $i = 1, 2, \dots, N$  do
    Step 4: Draw  $\mathbf{b}_i$  from  $p(\mathbf{b}_i | \phi_{(\gamma^*)}^*, \gamma^*, \beta, \mathbf{C}, \mathbf{V}, \tau, \Psi, \mathbf{L}, \mathbf{Y})$ 
  for  $k = 1, 2, \dots, K$  do
    Step 5: Draw  $\tau_k$  from  $p(\tau_k | \phi_{(\gamma^*)}^*, \gamma^*, \beta, \mathbf{b}, \mathbf{C}, \mathbf{V}, \Psi, \mathbf{L}, \mathbf{Y})$ 
  Step 6: Draw  $\Psi$  from  $p(\Psi | \phi_{(\gamma^*)}^*, \gamma^*, \beta, \mathbf{b}, \mathbf{C}, \mathbf{V}, \tau, \mathbf{L}, \mathbf{Y})$ ,
  for  $i = 1, 2, \dots, N$  do
    for  $j = 1, 2, \dots, n_i$  do
      Step 7: Draw  $L_{ij}$  from  $p(L_{ij} | \phi_{(\gamma^*)}^*, \gamma^*, \beta, \mathbf{b}, \mathbf{C}, \mathbf{V}, \tau, \Psi, \mathbf{Y})$ 
  for  $i = 1, 2, \dots, N$  do
    Step 8: Draw  $C_i$  from  $p(C_i | \phi_{(\gamma^*)}^*, \gamma^*, \beta, \mathbf{b}, \mathbf{V}, \tau, \Psi, \mathbf{L}, \mathbf{Y})$ 
  Step 9: Draw  $\beta$  from  $p(\beta | \phi_{(\gamma^*)}^*, \gamma^*, \mathbf{b}, \mathbf{C}, \mathbf{V}, \tau, \Psi, \mathbf{L}, \mathbf{Y})$ 
```

---

Then Steps 1 and 2 of Algorithm 1 are marginalized by using (10), while Step 3 of Algorithm 1 is marginalized by using (11). To maintain the target stationary distribution of Algorithm 1, the sampling steps are permuted in a specific order. Trimming is used to remove the redundant samples of components. One iteration of the PCG sampler is shown in Algorithm 2; refer to Park and van Dyk (2009); Jeong and Park (2016); Jeong et al. (2017); Park and Jeong (2018); Park et al. (2019) for more applications of the PCG sampler. Because the target stationary distribution of Algorithm 2 is maintained in a specific order, the change of the order of sampling steps may not guarantee the stationarity of a Markov chain, and care must be taken not to change the sampling order; refer to van Dyk and Park (2008). The details of Algorithm 2 are given in Appendix A.

#### 4. A Simulation Study

In this section, we validate the robustness and sensitivity of the proposed method through an extensive simulation study. Our results are based on a single dataset or 100 replicates, depending on the purpose.

#### 4.1. Simulation Setting

Throughout the simulation, we consider three subpopulation clusters of varying coefficients, and the total number  $N$  of subjects and the number of subjects in each cluster will be specified later based on simulation setups. The number  $n_i$  of observations for each subject  $i$  is randomly generated from  $\text{Poisson}(10) + 1$ . The values of an underlying effect modifier  $t$ ,  $\{t_{ij} : i = 1, \dots, N, j = 1, \dots, n_i\}$ , are randomly generated from a uniform distribution between 0 and 1, and the values of known covariates for subject  $i$ , i.e.,  $\mathbf{W}_i$ ,  $\mathbf{X}_i$ , and  $\mathbf{Z}_i$ , are independently generated from a standard normal distribution, except that the first column of both  $\mathbf{W}_i$  and  $\mathbf{Z}_i$  is set to a column vector of 1's. Within the range of  $t$  between 0 and 1,  $\alpha_{kl}(t)$  denotes a varying-coefficient function of the  $l$ th covariate in cluster  $k$ . The varying coefficients for three clusters are constant, linear, or nonlinear, as described below:

$$\begin{aligned}\alpha_{11}(t) &= 2 \exp\{-200(t - 0.2)^2\} + \exp\{-10(t - 0.6)^2\}, \\ \alpha_{12}(t) &= \sin(2\pi t^3), \\ \alpha_{21}(t) &= \sin\{8(t - 0.5)\} + 1.5 \exp\{-400(t - 0.5)^2\}, \\ \alpha_{22}(t) &= 2t, \\ \alpha_{31}(t) &= -2t, \\ \alpha_{32}(t) &= 0.\end{aligned}$$

The true values of the other model parameters are set to  $\boldsymbol{\beta} = (\beta_1, \beta_2)^\top = (1, -1)^\top$  and

$$\boldsymbol{\Psi} = \begin{pmatrix} \psi_{11} & \psi_{12} \\ \psi_{12} & \psi_{22} \end{pmatrix} = \begin{pmatrix} 0.5 & 0.25 \\ 0.25 & 0.8 \end{pmatrix}.$$

Then the latent response  $L_{ij}$  of the probit varying-coefficient mixed model is drawn from

$$L_{ij} \sim N\left(\mathbf{W}_i^{(j)} \boldsymbol{\alpha}_{C_i}^*(t_{ij}) + \mathbf{X}_i^{(j)} \boldsymbol{\beta} + \mathbf{Z}_i^{(j)} \mathbf{b}_i, 1\right), \quad i = 1, \dots, N, \quad j = 1, \dots, n_i,$$

which is used to generate a series of binary data such that  $Y_{ij} = I(L_{ij} > 0)$  for observation  $j$  on subject  $i$ .

#### 4.2. Comparison with a Single Population Model

For the analysis of longitudinal binary data, Jeong et al. (2017) proposed a Bayesian method for a probit varying-coefficient mixed model without a heterogeneous subpopulation assumption. We evaluate the validity of our subgroup modeling by comparing their approach to ours, where data come from distinct subpopulations. Both methods use a dataset generated from the simulation setup described in Section 4.1, where each of three clusters has 400 subjects, resulting in  $N = 1200$  subjects in total. For each varying coefficient, we use  $M_l = 30$  knot-candidates chosen by the sample quantiles of the effect modifier  $t$ .

The proposed PCG sampler begins with three distinct sets of initial parameter values that are over-dispersed. With 10000 iterations through a label switching algorithm (Papastamoulis and Iliopoulos, 2010), we quantitatively examine the convergence of the

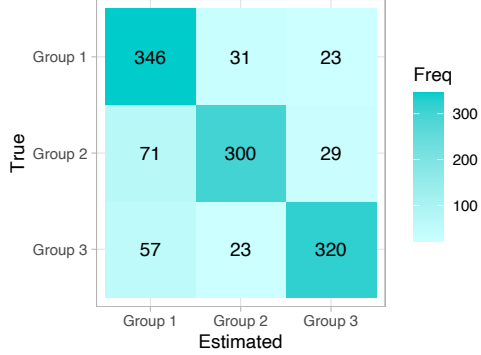


Figure 1: A confusion matrix for functional clustering for the true clusters and estimated clusters.

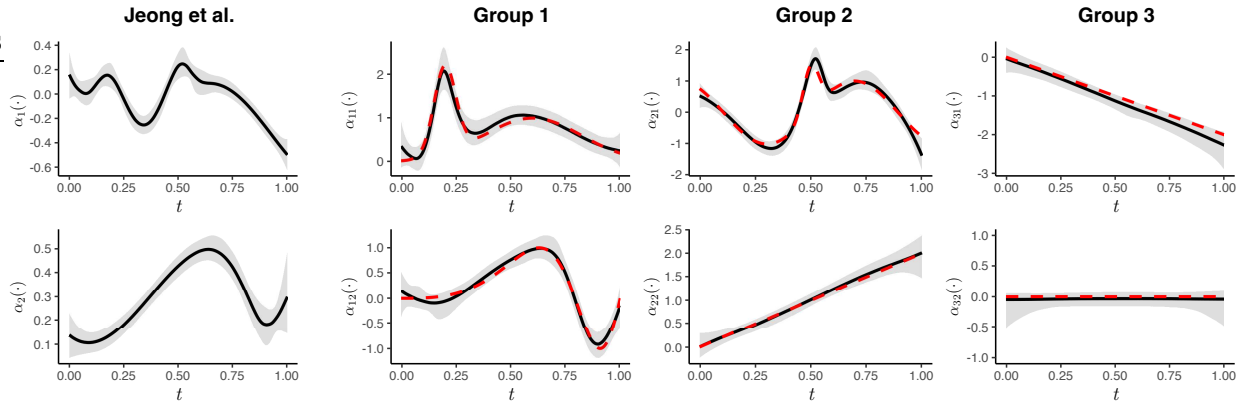


Figure 2: Posterior summaries of varying-coefficients: true functions (dotted red lines), posterior medians (solid black lines) and point-wise 95% posterior intervals (gray areas). The first column shows the posteriors of the varying-coefficients estimated by Jeong et al. (2017), and the next three columns show the cluster-specific posteriors of the varying-coefficients obtained by the proposed method.

sampler with the  $R^{1/2}$  diagnostic (Gelman and Rubin, 1992) for the fixed-dimensional parameters and the fixed points of the varying coefficients. Because all  $R^{1/2}$  statistics are confirmed below 1.1, we combine the second halves of the three chains thinned by taking every 5th sample, and our posterior inference is based on the resulting 3000 mixed samples.

Table 1 shows a confusion matrix for functional clustering performed by our subgroup modeling approach. The membership of each subject is taken to be the most frequent cluster out of the posterior samples. The clustering accuracy is roughly 80.5%. Figure 2 shows posterior summaries of the varying-coefficients obtained by Jeong et al. (2017) and the proposed method. With our clustering-based approach, each varying-coefficient function is precisely estimated by the corresponding point-wise posterior median and well covered by the corresponding point-wise 95% credible bands; the coverage of the credible bands will be examined in Section 4.3. By contrast, the curves estimated by Jeong et al. (2017) are clearly far from each of the true functions, and rather the estimated curve is close to the true functions averaged across the clusters. Table 1 shows that ignoring subpopulation effects

Table 1: Posterior Quantiles of Fixed Dimensional Parameters

Parameter	True	Jeong et al. (2017)			Proposed method		
		2.5%	50%	97.5%	2.5%	50%	97.5%
$\beta_1$	1	0.750	0.789	0.827	0.958	1.009	1.064
$\beta_2$	-1	-0.864	-0.824	-0.785	-1.11	-1.051	-0.995
$\psi_{11}$	0.50	0.671	0.769	0.881	0.428	0.536	0.654
$\psi_{12}$	0.25	0.145	0.211	0.282	0.234	0.319	0.419
$\psi_{22}$	0.80	0.444	0.525	0.616	0.705	0.836	0.997

results in a significant bias for model parameters including the varying coefficients.

#### 4.3. Sensitivity Analysis

In this section, we examine how sensitive the proposed method is to the sample size and the concentration parameter of the DP prior. We consider three different scenarios for a sample size: Scenario I, where each cluster has 400 subjects ( $N = 1200$ ), Scenario II, where each cluster has 200 subjects ( $N = 600$ ), and Scenario III, where the three clusters have 600, 400, and 200 subjects, respectively ( $N = 1200$ ). For each scenario, three different values of the concentration parameter are also considered:  $\nu = 0.1, 1$ , and  $10$ . The proposed method is applied to each combination of the scenarios for the sample size and the concentration parameter with 100 replications of the datasets. Starting with dispersed initial values, we collect 10000 posterior samples with sufficient convergence based on the  $R^{1/2}$  diagnostic.

The side-by-side boxplots in Figure 3 illustrate clustering performance for the 100 replicated datasets in terms of precision, recall, and F1-score. The clusters with a larger sample size perform better in clustering, as expected. The metrics are similar across different values of  $\nu$ , indicating that clustering performance is not highly affected by the concentration parameter. This concludes that our clustering procedure is robust to specification of the hyperparameter. We also calculate the coverage probabilities of the point-wise 95% credible bands with the 100 replicates. Figure 4 shows that the coverage probabilities are close enough to 0.95, validating the uncertainty quantification through the posterior distribution. In particular, the coverage probabilities are similar enough for different values of  $\nu$ , providing further evidence for robustness against the hyperparameter specification. Figure 5 overlays the point-wise posterior medians of the varying coefficients of the 100 replicated datasets with the default choice  $\nu = 1$ . It is clear that the estimated posterior medians are closer to the true functions with larger sample sizes. The posterior medians obtained with  $\nu = 0.1$  and  $\nu = 10$  are also similar and thus omitted.

Figure 3 shows the side-by-side boxplots of clustering performance for the 100 replicated datasets in terms of precision, recall, and F1-score. As expected, clusters with a larger sample size perform better in functional clustering. The metrics are similar across different values of  $\nu$ , indicating that the concentration parameter has little effect on clustering performance. This means that our clustering procedure is robust to the specification of the hyperparameter. With the 100 replicates, we also calculate the coverage probabilities of the

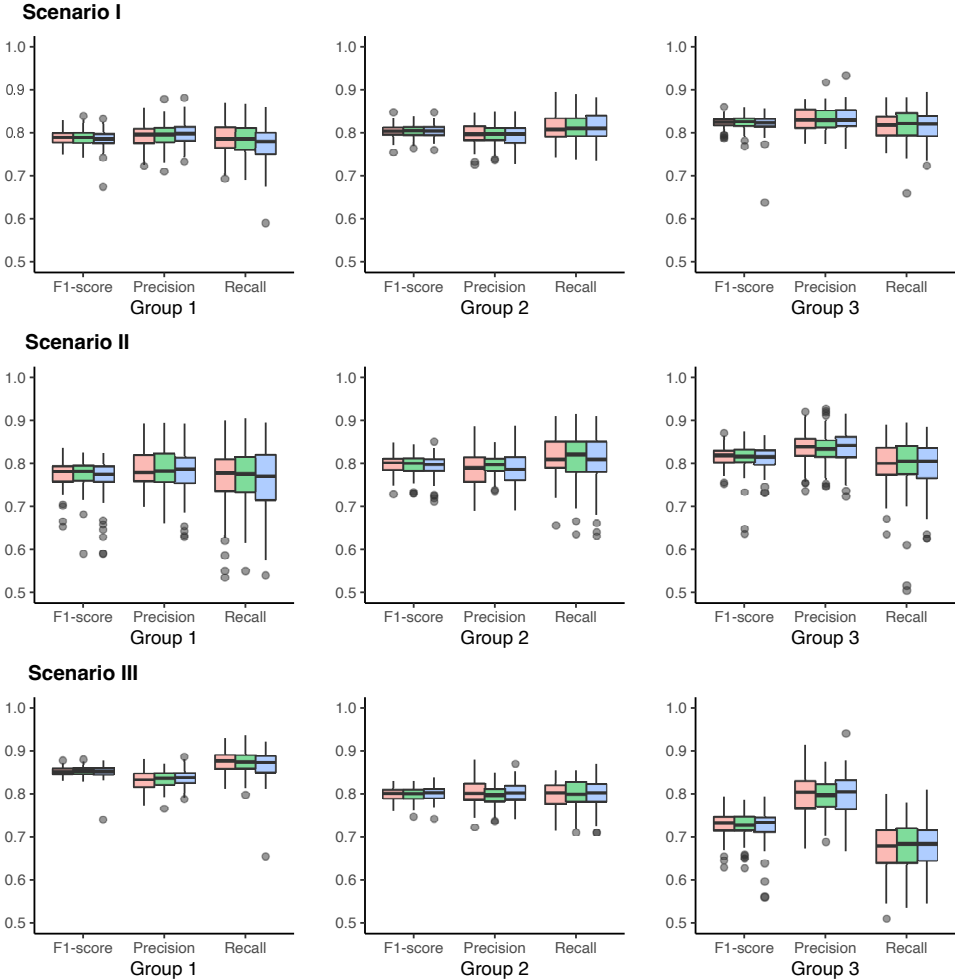


Figure 3: Performance measures for the clustering procedure over 100 replicated datasets with  $\nu = 0.1$  (red),  $\nu = 1$  (green), and  $\nu = 10$  (blue).

point-wise 95% credible intervals. Figure 4 shows that the coverage probabilities are close to 0.95, validating the quantification of posterior uncertainty. The coverage probabilities, in particular, are similar enough for different values of  $\nu$ , thereby showing additional evidence for robustness against the hyperparameter specification. Figure 5 shows the point-wise posterior medians of the varying coefficients for the 100 replicated datasets with the default choice of  $\nu = 1$ , along with the true varying-coefficient functions. With larger sample sizes, the estimated posterior medians are clearly closer to the true functions. Such results are quite similar with the cases of  $\nu = 0.1$  and  $\nu = 10$ , so they are omitted for brevity.

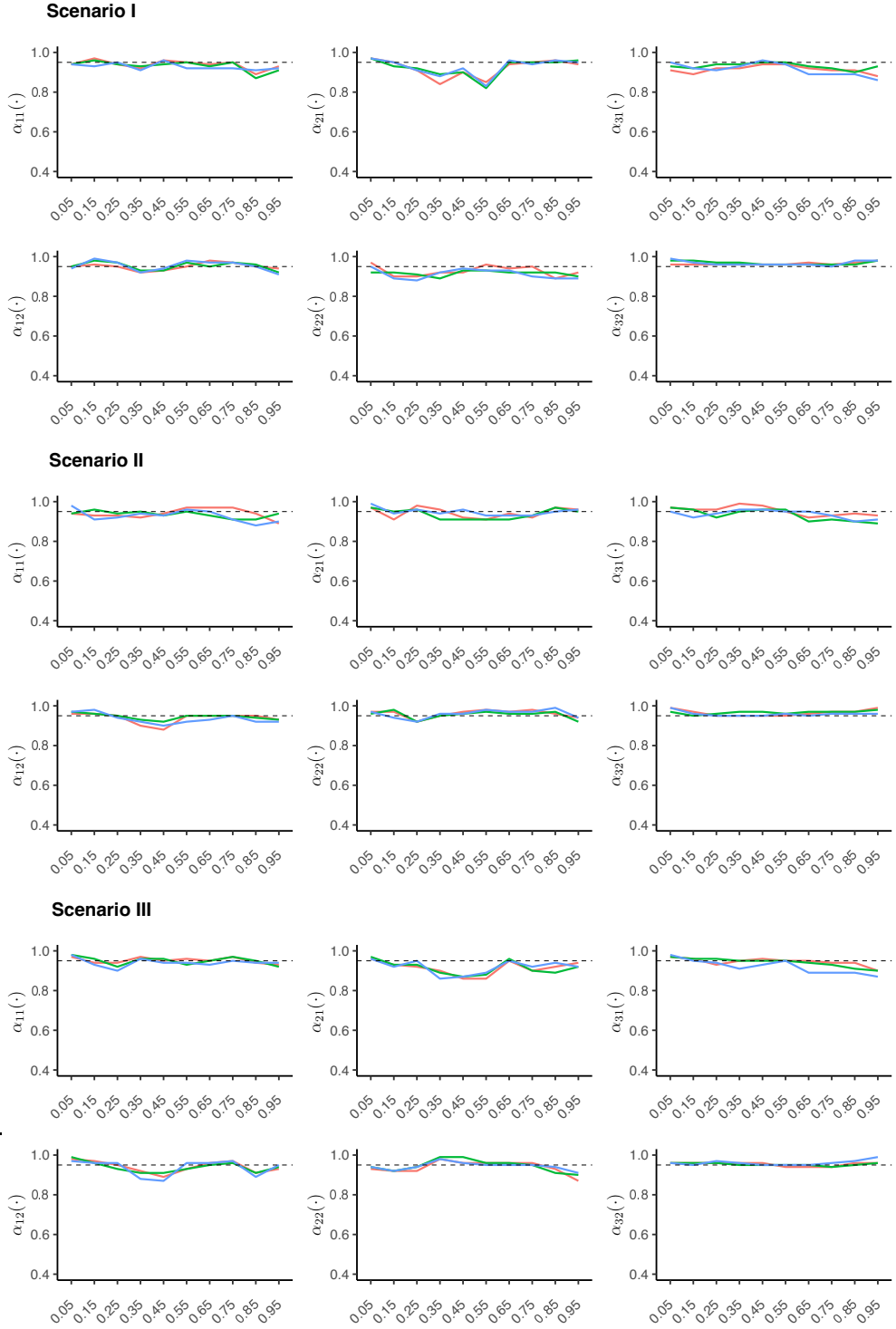
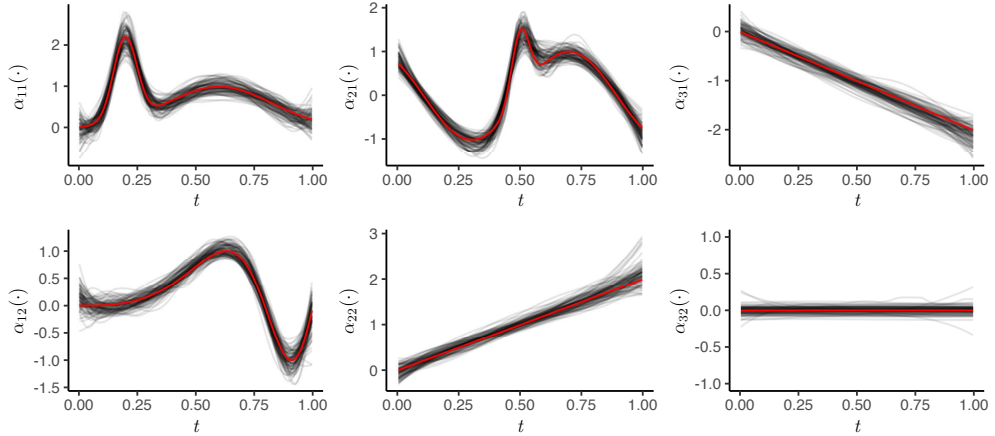
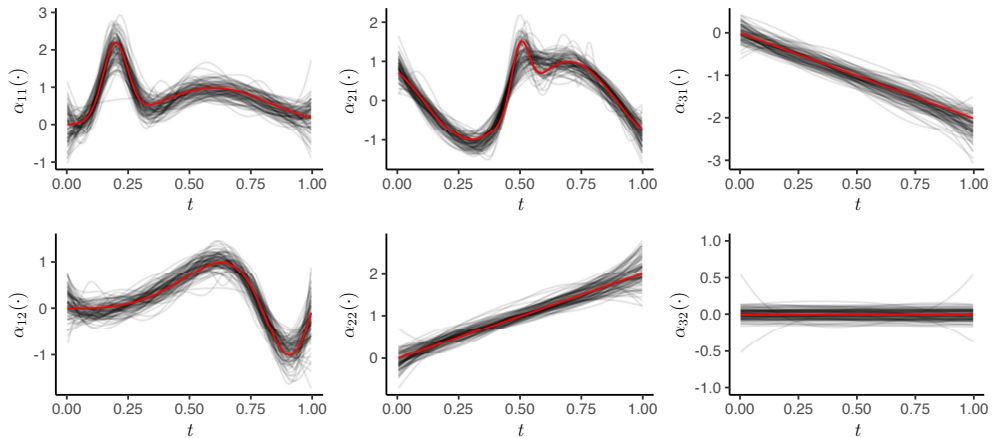


Figure 4: Coverage probabilities of the varying-coefficient functions obtained from 100 replicated datasets with  $\nu = 0.1$  (red),  $\nu = 1$  (green), and  $\nu = 10$  (blue).

### Scenario I



### Scenario II



### Scenario III

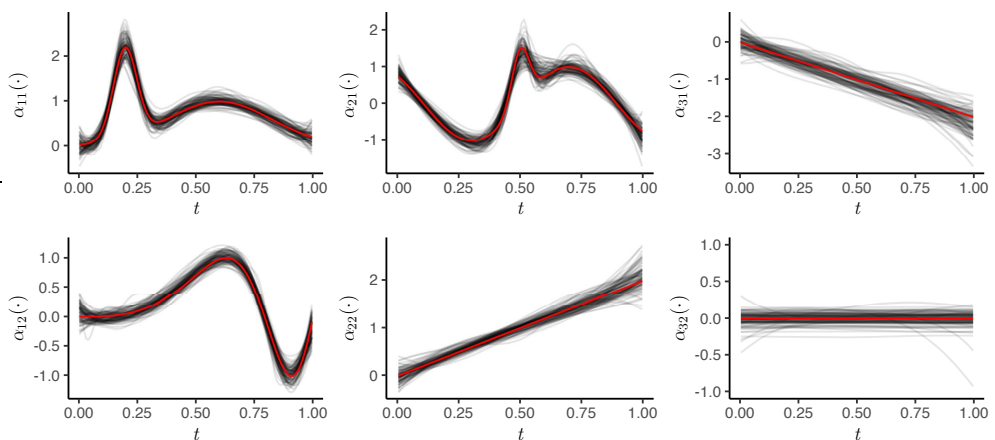


Figure 5: The point-wise posterior medians of varying coefficients of the 100 replicated datasets (gray solid lines) and the true varying-coefficient functions (red solid lines).

Table 2: Characteristics of the Clustered Groups

Covariate	Overall	Group 1	Group 2
Female	35.1%	33.3%	89.1%
Married	57.7%	55.9%	71.2%
White-collar workers	38.7%	41.1 %	20.8%
Civil servants	25.8%	29.0%	4.0%
University	57.2%	58.4%	42.0%

## 5. Application to Binary Longitudinal Data

### 5.1. Data Description and Modeling Procedure

In this section, we consider the German Socioeconomic Panel (GSOEP) data (Riphahn et al., 2003). The dataset consists of repeated observations from 7293 subjects in Germany for the years 1984–1988, 1991, and 1994. The response variable of interest is working status (employed=1; otherwise=0) and covariates consist of  $A_{ij}$  (age),  $M_{ij}$  (marital status; married=1, otherwise=0),  $K_{ij}$  (children under the age of 16 in the household; yes=1, no=0),  $H_{ij}$  (degree of handicap; 0 to 100 in percent), and  $S_{ij}$  (personal health satisfaction; 0 to 10). We confine our samples to 893 subjects under the age of 53 with Abitur degrees in order to examine the varying effect of having young children in the household on working status as a function of age for people with secondary education.

According to our preliminary analysis, which assumes varying effects for all covariates, we have decided to treat handicap, personal health satisfaction, and marital status as constant effects in subsequent analyses. As a result, we aim to model the varying effects of the intercept and the presence of children under the age of 16, while treating the remaining covariates as fixed effects. Our target model is then given by

$$L_{ij} = \alpha_{C_i 0}^*(A_{ij}) + \alpha_{C_i K}^*(A_{ij})K_{ij} + \beta_M M_{ij} + \beta_S S_{ij} + \beta_H H_{ij} + b_i + \epsilon_{ij}.$$

The reduced model complexity based on the preliminary analysis leads to faster computation and greater stability.

Similar to Section 4.2, we compare the proposed method with the model in Jeong et al. (2017) that ignores heterogeneity among subjects. The corresponding simple model is given by

$$L_{ij} = \alpha_0(A_{ij}) + \alpha_K(A_{ij})K_{ij} + \beta_M M_{ij} + \beta_S S_{ij} + \beta_H H_{ij} + b_i + \epsilon_{ij}.$$

As shown in the next section, the simple model fails to account for heterogeneity among samples and can be obtained by pooling the results of the proposed target model.

### 5.2. Analysis and Results

We ran the proposed PCG sampler with three over-dispersed initial values. Figure 6 shows the convergence characteristics of the sampler by using the  $R^{1/2}$  diagnostic for the

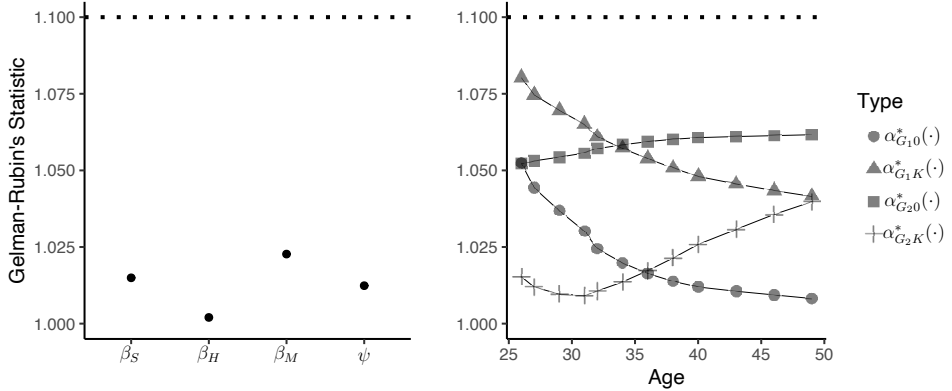


Figure 6: The  $R^{1/2}$  statistics for the fixed-dimensional parameters (left) and the fixed points of the varying coefficients (right).

Table 3: Posterior Summaries of the Fixed-Dimensional Parameters

Parameter	Jeong et al. (2017)			Proposed method		
	Mean	Median	95% interval	Mean	Median	95% interval
$\psi$	3.949	3.893	(3.031, 5.106)	3.539	3.357	(1.573, 6.334)
$\beta_S$	0.006	0.006	(-0.051, 0.063)	0.016	0.016	(-0.065, 0.097)
$\beta_H$	-0.010	-0.010	(-0.026, 0.006)	-0.002	-0.002	(-0.023, 0.020)
$\beta_M$	0.299	0.297	(-0.041, 0.647)	0.292	0.284	(-0.178, 0.793)

fixed-dimensional parameters and the fixed points of the varying coefficients. Because all  $R^{1/2}$  statistics are below 1.1, we combine the second halves of three chains each with 150000 iterations through a label switching algorithm. Then, after thinning every 50th sample, our posterior inference is based on 4500 mixed samples.

Our posterior analysis suggests two major groups, as well as a few minor groups that can be combined to form a single group. The largest cluster, Group 1, accounts for 89.4% of subjects, the second largest, Group 2, accounts for 7.2%, and the remaining clusters account for 3.4%. Some characteristics of the two major groups are summarized in Table 2, demonstrating that these groups are made up of heterogeneous subjects. Specifically, Group 1 has a much lower proportion of females who tend to be more responsible for parenting than Group 2. In addition, Group 1 has a higher proportion of white-collar workers, civil servants, and university graduates with high job security than Group 2. Such difference in characteristics results in the different posterior estimates of varying-coefficient functions, as shown in Figure 7.

Figure 7 shows the posterior summaries of the varying-coefficient functions resulting from functional clustering. The first row of Figure 7 corresponds to the group-level varying-intercept functions. The intercept function of Group 1 is significantly positive and keeps increasing up to early 50s, implying that a posterior probability of being employed becomes higher as one tends to be old while holding all covariates constant. In contrast, Group 2 has

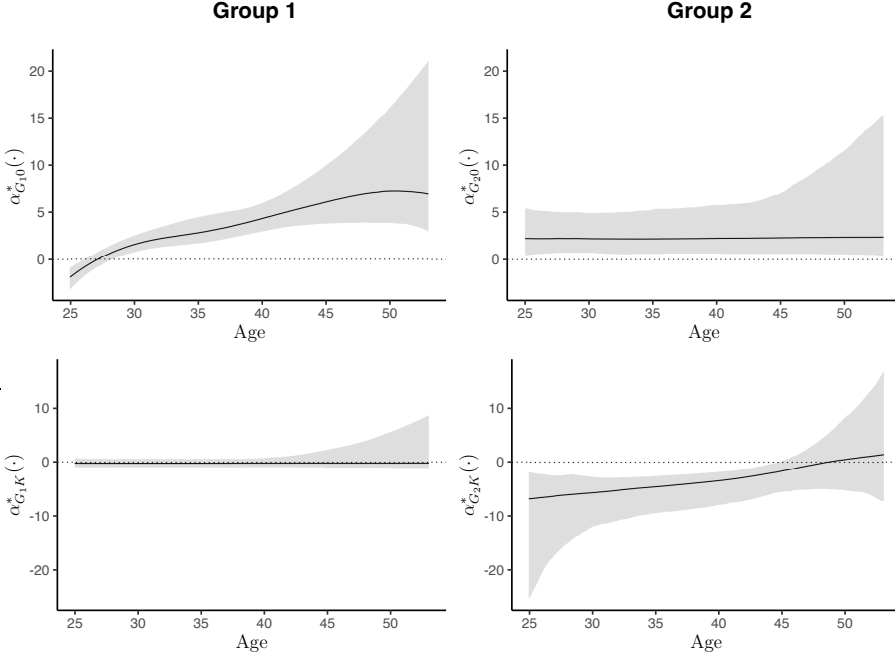


Figure 7: Posterior summaries of varying coefficients for two major groups. Solid lines represent the point-wise posterior medians of each varying coefficient function and gray regions correspond to point-wise 95% posterior intervals.

a slightly positive but constant intercept function in all ages. The second row of Figure 7 shows the varying-coefficient function for having children below age 16 in the household. The 95% point-wise posterior intervals for Group 1 includes 0, which implies that having children below age 16 in the household does not significantly affect the probability of employment. Unlike Group 1, the existence of young children in Group 2’s household significantly decreases the probability of employment until his/her mid 40s. The probability is further decreased when the employee’s age tends to be younger. This is due in part to the fact that Group 2 has a higher proportion of females than Group 1, and females were more responsible for child care in the late twentieth century.

Table 3 shows the posterior summaries of fixed-dimensional parameters, where  $\text{Var}(b_i) = \psi$  represents the variance of a random effect, and  $\beta_H$ ,  $\beta_S$ , and  $\beta_M$  represent the coefficients of fixed effects,  $H_{ij}$ ,  $S_{ij}$ , and  $M_{ij}$ , respectively. Based on the fact that the 95% posterior intervals include zero, we decide that the fixed effects have no significant influence on the employment status when the varying effects of having young children in the household for heterogeneous subpopulations are accounted for in the model. When the heterogeneous subpopulation assumption is ignored, the results obtained by Jeong et al. (2017) appear to be similar, but with narrower 95% credible intervals. This is due to the fact that Jeong et al. (2017) does not fully account for the variability of heterogeneous subpopulations.

Our proposed method identifies two major subpopulations with different characteristics, as shown in Table 2, and these subpopulations show different age-varying effects of hav-

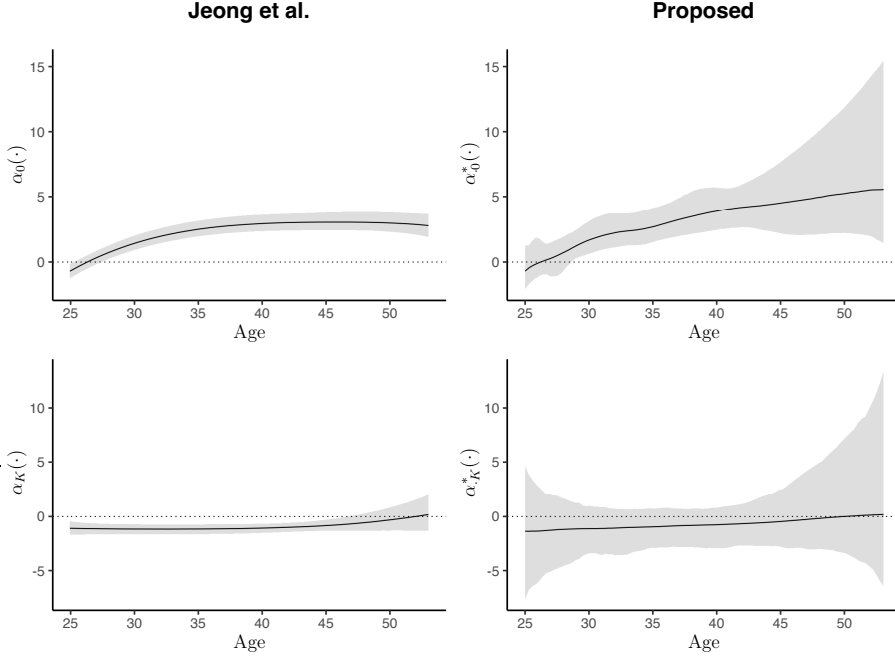


Figure 8: The first column shows the posterior summaries of the varying coefficients obtained by Jeong et al. (2017), and the second column is with respect to the proposed method pooled by the weights corresponding to cluster assignments, with posterior medians (solid lines) and point-wise 95% posterior intervals (gray areas).

ing young children in a household on working status, as illustrated in Figure 7. When the heterogeneous subpopulation assumption is ignored, however, the single population model proposed by Jeong et al. (2017) estimates the varying-coefficient functions applied to the entire population, as shown in the first column of Figure 8. In the presence of heterogeneous subpopulations, such an approach would fail to separate subpopulations with different characteristics, leading to erroneous conclusions. This is confirmed by producing the pooled varying-coefficient functions estimated by the proposed method, as shown in the second column of Figure 8. These findings demonstrate the proposed model’s validity and utility in accounting for a heterogeneous population.

## 6. Discussion

In this paper, we propose a functional clustering method for a heterogeneous series of binary data. Our proposed method can capture the varying effects of covariates on a series of binary responses as a function of an effect modifier, while accounting for heterogeneity among subjects by functional clustering and random effects. By doing so, we extract population-level fixed effects, cluster-level varying effects, and subject-level random effects. Under the unknown number of clusters, the proposed method correctly estimates cluster-specific varying-coefficients without the risk of overfitting caused by using a large number of knots in a regression spline. For functional clustering, we propose to use the Dirichlet

process to be free from specifying the exact number of clusters in advance. For posterior inference, we carefully devise a PCG sampler by specifying appropriate prior distributions and marginalizing some model components out of the model. The resulting PCG sampler allows efficient knot selection for the unknown varying-coefficient functions, which can be generalized to model selection problems.

## Appendix A. Details of Algorithm 2,

In this section, we describe the details of Algorithm 2. Let  $\mathcal{C}_d$  denote a set of clusters containing at least one subject and let  $\mathcal{C}_d^c$  denote a set of clusters containing no subject, in the  $d$ th sampling iteration. For  $d$ th iteration:

**Step 1:** Draw  $\gamma_{kl}^*$  from  $p(\gamma_{kl}^* | \gamma_{-kl}^*, \beta, \mathbf{C}, \mathbf{V}, \tau, \Psi, \mathbf{L}, \mathbf{Y})$  that is a Bernoulli with success probability

$$\frac{f(\gamma_{kl}^* = 1, \gamma_{-kl}^*)}{f(\gamma_{kl}^* = 1, \gamma_{-kl}^*) + f(\gamma_{kl}^* = 0, \gamma_{-kl}^*)}, \quad k \in \mathcal{C}_d, \quad l = 1, \dots, p,$$

where  $\gamma_{-kl}^*$  denotes all latent indicator variables except  $\gamma_{kl}^*$  in  $\gamma_k^*$ ,

$$\begin{aligned} f(\gamma_{kl}^*, \gamma_{-kl}^*) &= B(|\gamma_{kl}^*| + a, M_l + 1 - |\gamma_{kl}^*| + b) \times \det \left( \tau_k \mathbf{R}_{k(\gamma_k^*)}^{-1} \Xi_{k(\gamma_k^*, \mathbf{C}, \Psi)} + \mathbf{I}_{|\gamma_k^*|} \right)^{-1/2} \\ &\quad \times \exp \left\{ \frac{1}{2} \xi_{k(\gamma_k^*, \mathbf{C}, \Psi, \mathbf{L}, \beta)}^\top \left( \Xi_{k(\gamma_k^*, \mathbf{C}, \Psi)} + \tau_k^{-1} \mathbf{R}_{k(\gamma_k^*)} \right)^{-1} \xi_{k(\gamma_k^*, \mathbf{C}, \Psi, \mathbf{L}, \beta)} \right\}, \\ \Xi_{k(\gamma_k^*, \mathbf{C}, \Psi)} &= \sum_{i:C_i=k} \mathbf{W}_{i(\gamma_k^*)}^{\star\top} \left( \mathbf{I}_{n_i} + \mathbf{Z}_i \Psi \mathbf{Z}_i^\top \right)^{-1} \mathbf{W}_{i(\gamma_k^*)}^\star, \\ \xi_{k(\gamma_k^*, \mathbf{C}, \Psi, \mathbf{L}, \beta)} &= \sum_{i:C_i=k} \mathbf{W}_{i(\gamma_k^*)}^{\star\top} \left( \mathbf{I}_{n_i} + \mathbf{Z}_i \Psi \mathbf{Z}_i^\top \right)^{-1} (\mathbf{L}_i - \mathbf{X}_i \beta), \end{aligned}$$

and  $\mathbf{I}_{|\gamma_k^*|}$  and  $\mathbf{I}_{n_i}$  are identity matrices whose sizes of each dimension are  $|\gamma_k^*|$  and  $n_i$ , respectively. In the case of  $k \in \mathcal{C}_d^c$ ,  $\gamma_{kl}^*$  is drawn from its prior distribution because  $\Xi_{k(\gamma_k^*, \mathbf{C}, \Psi)}$  and  $\xi_{k(\gamma_k^*, \mathbf{C}, \Psi, \mathbf{L}, \beta)}$  do not exist.

**Step 2:** Draw  $V_k$  from  $p(V_k | \gamma^*, \beta, \mathbf{C}, \tau, \Psi, \mathbf{L}, \mathbf{Y})$  that is a beta, i.e.,

$$V_k | (\gamma^*, \beta, \mathbf{C}, \tau, \Psi, \mathbf{L}, \mathbf{Y}) \sim \text{Beta} \left( 1 + m_k, \nu + \sum_{h=k+1}^K m_h \right), \quad k = 1, \dots, K-1,$$

where  $m_k = \sum_{i=1}^N I(C_i = k)$ .

**Step 3:** Draw  $\phi_{(\gamma_k^*)}^*$  from  $p(\phi_{(\gamma_k^*)}^* | \gamma^*, \beta, \mathbf{C}, \mathbf{V}, \tau, \Psi, \mathbf{L}, \mathbf{Y})$  that is a multivariate normal distribution, i.e.,

$$\begin{aligned} \phi_{(\gamma_k^*)}^* | (\gamma^*, \beta, \mathbf{C}, \mathbf{V}, \tau, \Psi, \mathbf{L}, \mathbf{Y}) &\sim N_{|\gamma_k^*|} \left( \left( \Xi_{k(\gamma_k^*, \mathbf{C}, \Psi)} + \tau_k^{-1} \mathbf{R}_{k(\gamma_k^*)} \right)^{-1} \xi_{k(\gamma_k^*, \mathbf{C}, \Psi, \mathbf{L}, \beta)}, \left( \Xi_{k(\gamma_k^*, \mathbf{C}, \Psi)} + \tau_k^{-1} \mathbf{R}_{k(\gamma_k^*)} \right)^{-1} \right), \quad k \in \mathcal{C}_d, \end{aligned}$$

and

$$\phi_{(\gamma_k^*)}^* | (\gamma^*, \beta, \mathbf{C}, \mathbf{V}, \tau, \Psi, \mathbf{L}, \mathbf{Y}) \sim N_{|\gamma_k^*|} \left( \mathbf{0}, \tau_k \mathbf{R}_{k(\gamma_k^*)}^{-1} \right), \quad k \in \mathcal{C}_d^c.$$

**Step 4:** Draw  $\mathbf{b}_i$  from  $p(\mathbf{b}_i | \phi_{(\gamma^*)}^*, \gamma^*, \beta, \mathbf{C}, \mathbf{V}, \tau, \Psi, \mathbf{L}, \mathbf{Y})$  that is multivariate normal, i.e.,

$$\mathbf{b}_i | (\phi_{(\gamma^*)}^*, \gamma^*, \beta, \mathbf{C}, \mathbf{V}, \tau, \Psi, \mathbf{L}_i, \mathbf{Y}) \sim N_r \left( \mathbf{U}_{i(\Psi, \phi_{(\gamma^*)}^*, \gamma_{C_i}^*, \mathbf{L}, \beta)}, \mathbf{A}_{(\Psi)} \right), \quad i = 1, \dots, N,$$

where

$$\begin{aligned} \mathbf{U}_{i(\Psi, \phi_{(\gamma^*)}^*, \gamma_{C_i}^*, \mathbf{L}_i, \beta)} &= \Psi \mathbf{Z}_i^\top (\mathbf{I}_{n_i} + \mathbf{Z}_i \Psi \mathbf{Z}_i^\top)^{-1} (\mathbf{L}_i - \mathbf{W}_{i(\gamma_{C_i}^*)}^* \phi_{(\gamma_{C_i}^*)}^* - \mathbf{X}_i \beta), \\ \mathbf{A}_{(\Psi)} &= \Psi - \Psi \mathbf{Z}_i^\top (\mathbf{I}_{n_i} + \mathbf{Z}_i \Psi \mathbf{Z}_i^\top)^{-1} \mathbf{Z}_i \Psi. \end{aligned}$$

**Step 5:** Draw  $\tau_k$  from  $p(\tau_k | \phi_{(\gamma^*)}^*, \gamma^*, \beta, \mathbf{b}, \mathbf{C}, \mathbf{V}, \Psi, \mathbf{L}, \mathbf{Y})$  that is an inverse gamma, i.e.,

$$\begin{aligned} \tau_k | (\phi_{(\gamma^*)}^*, \gamma^*, \beta, \mathbf{b}, \mathbf{C}, \mathbf{V}, \Psi, \mathbf{L}, \mathbf{Y}) & \\ \sim \text{IG} \left( \frac{1 + |\gamma_k^*|}{2}, \frac{N + \phi_{(\gamma_k^*)}^{*\top} \mathbf{R}_{k(\gamma_k^*)} \phi_{(\gamma_k^*)}^*}{2} \right), \quad k &= 1, \dots, K. \end{aligned}$$

**Step 6:** Draw  $\Psi$  from  $p(\Psi | \phi_{(\gamma^*)}^*, \gamma^*, \beta, \mathbf{b}, \mathbf{C}, \mathbf{V}, \tau, \mathbf{L}, \mathbf{Y})$  that is an inverse Wishart,

$$\Psi \sim \text{IW} \left( u + N, \mathbf{D} + \sum_{i=1}^N \mathbf{b}_i \mathbf{b}_i^\top \right).$$

**Step 7:** Draw  $L_{ij}$  from  $p(L_{ij} | \phi_{(\gamma^*)}^*, \gamma^*, \beta, \mathbf{b}, \mathbf{C}, \mathbf{V}, \tau, \Psi, \mathbf{Y})$  that is truncated normal, i.e.,

$$L_{ij} | (\phi_{(\gamma^*)}^*, \gamma^*, \beta, \mathbf{b}, \mathbf{C}, \mathbf{V}, \tau, \Psi, \mathbf{Y}) \sim \begin{cases} \text{TN}_{(-\infty, 0]}(\mu_{C_i}^{(j)}, 1) & \text{if } Y_{ij} = 0 \\ \text{TN}_{(0, \infty)}(\mu_{C_i}^{(j)}, 1) & \text{if } Y_{ij} = 1 \end{cases}, \quad i = 1, \dots, N, \quad j = 1, \dots, n_i,$$

where  $\mu_{C_i}^{(j)}$  denotes the  $j$ th element of  $\mu_{C_i} = \mathbf{W}_{i(\gamma_{C_i}^*)}^* \phi_{(\gamma_{C_i}^*)}^* + \mathbf{X}_i \beta + \mathbf{Z}_i \mathbf{b}_i$ .

**Step 8:** Draw  $C_i$  from  $p(C_i | \phi_{(\gamma^*)}^*, \gamma^*, \beta, \mathbf{b}, \mathbf{V}, \tau, \Psi, \mathbf{L}, \mathbf{Y})$  that has a discrete distribution with probabilities

$$P(C_i = k | (\phi_{(\gamma^*)}^*, \gamma^*, \beta, \mathbf{b}, \mathbf{V}, \tau, \Psi, \mathbf{L}, \mathbf{Y})) \propto \frac{\pi_k(\mathbf{V}) N_{n_i}(\mathbf{L}_i; \mu_k, \mathbf{I}_{n_i})}{\sum_{k=1}^K \pi_k(\mathbf{V}) N_{n_i}(\mathbf{L}_i; \mu_k, \mathbf{I}_{n_i})}, \quad k = 1, \dots, K,$$

where  $\mu_k = \mathbf{W}_{i(\gamma_k^*)}^* \phi_{(\gamma_k^*)}^* + \mathbf{X}_i \beta + \mathbf{Z}_i \mathbf{b}_i$ .

**Step 9:** Draw  $\beta$  from  $p(\beta | \phi_{(\gamma^*)}^*, \gamma^*, \mathbf{b}, \mathbf{C}, \mathbf{V}, \tau, \Psi, \mathbf{L}, \mathbf{Y})$  that is multivariate normal, i.e.,

$$\beta | (\phi_{(\gamma^*)}^*, \gamma^*, \mathbf{b}, \mathbf{C}, \mathbf{V}, \tau, \Psi, \mathbf{L}, \mathbf{Y}) \sim N_q \left( \Delta^{-1} \sum_{i=1}^N \mathbf{X}_i^\top (\mathbf{L}_i - \mathbf{W}_{i(\gamma_{C_i}^*)}^* \phi_{(\gamma_{C_i}^*)}^* - \mathbf{Z}_i \mathbf{b}_i), \Delta^{-1} \right),$$

where  $\Delta = \mathbf{P}^{-1} + \sum_{i=1}^N \mathbf{X}_i^\top \mathbf{X}_i$ .

## Appendix B. R package fvcc

We provide an R package called `fvcc` for the proposed model. The package can be installed with the `devtools` package available in CRAN as follows.

```
devtools::install_github("jwsohn612/fvcc")
library(fvcc)
help(fvcc)
```

The main function `fvcc` contains a code script for reproducing the simulation results in Section 4.

## Acknowledgements

S. Jeong's research was supported by the Yonsei University Research Fund of 2022-22-0097. T. Park's research was supported by Basic Science Research Program through the National Research Foundation of Korea(NRF) funded by the Ministry of Education (2017R1D1A1B03033536) and by the National Research Foundation of Korea(NRF) grant funded by the Korea government(MSIT) (2020R1A2C1A01005949).

## References

R. Stiratelli, N. Laird, J. H. Ware, Random-effects models for serial observations with binary response, *Biometrics* (1984) 961–971. doi:10.2307/2531147.

C. Varin, C. Czado, A mixed autoregressive probit model for ordinal longitudinal data, *Biostatistics* 11 (2009) 127–138. doi:10.1093/biostatistics/kxp042.

M. W. Guerra, J. Shults, J. Amsterdam, T. Ten-Have, The analysis of binary longitudinal data with time-dependent covariates, *Statistics in Medicine* 31 (2012) 931–948. doi:10.1002/sim.4465.

T. Hastie, R. Tibshirani, Varying-coefficient models, *Journal of the Royal Statistical Society. Series B (Methodological)* (1993) 757–796. doi:10.1111/j.2517-6161.1993.tb01939.x.

D. R. Hoover, J. A. Rice, C. O. Wu, L.-P. Yang, Nonparametric smoothing estimates of time-varying coefficient models with longitudinal data, *Biometrika* 85 (1998) 809–822. doi:10.1093/biomet/85.4.809.

C. O. Wu, C.-T. Chiang, D. R. Hoover, Asymptotic confidence regions for kernel smoothing of a varying-coefficient model with longitudinal data, *Journal of the American Statistical Association* 93 (1998) 1388–1402. doi:10.1080/01621459.1998.10473800.

S. Lang, A. Brezger, Bayesian p-splines, *Journal of Computational and Graphical Statistics* 13 (2004) 183–212. doi:10.1198/1061860043010.

Y. Sun, H. Wu, Semiparametric time-varying coefficients regression model for longitudinal data, *Scandinavian Journal of Statistics* 32 (2005) 21–47. doi:10.1111/j.1467-9469.2005.00413.x.

J. Fan, W. Zhang, Statistical methods with varying coefficient models, *Statistics and its Interface* 1 (2008) 179. doi:10.4310/sii.2008.v1.n1.a15.

Y. Lu, R. Zhang, Smoothing spline estimation of generalised varying-coefficient mixed model, *Journal of Nonparametric Statistics* 21 (2009) 815–825. doi:10.1080/10485250903151078.

S. Jeong, T. Park, Bayesian semiparametric inference on functional relationships in linear mixed models, *Bayesian Analysis* 11 (2016) 1137–1163. doi:10.1214/15-BA987.

S. Jeong, M. Park, T. Park, Analysis of binary longitudinal data with time-varying effects, *Computational Statistics & Data Analysis* 112 (2017) 145–153. doi:10.1016/j.csda.2017.03.007.

T. Park, S. Jeong, Analysis of poisson varying-coefficient models with autoregression, *Statistics* 52 (2018) 34–49. doi:10.1080/02331888.2017.1353514.

W. Shen, S. Ghosal, Adaptive bayesian procedures using random series priors, *Scandinavian Journal of Statistics* 42 (2015) 1194–1213.

R. M. Neal, Regression and classification using gaussian process priors, *Bayesian Statistics* 6 (1998) 475.

M. Smith, R. Kohn, Nonparametric regression using bayesian variable selection, *Journal of Econometrics* 75 (1996) 317–343. doi:10.1016/0304-4076(95)01763-1.

I. DiMatteo, C. R. Genovese, R. E. Kass, Bayesian curve-fitting with free-knot splines, *Biometrika* 88 (2001) 1055–1071. doi:10.1093/biomet/88.4.1055.

R. Kohn, M. Smith, D. Chan, Nonparametric regression using linear combinations of basis functions, *Statistics and Computing* 11 (2001) 313–322. doi:10.1023/A:1011916902934.

D. Ruppert, M. P. Wand, R. J. Carroll, *Semiparametric Regression*, 12, Cambridge University Press, 2003.

J. O. Ramsey, B. W. Silverman, *Functional data analysis*, Springer Series in Statistics, New York: Springer Verlag (2005).

C. Aßmann, J. Boysen-Hogrefe, A Bayesian approach to model-based clustering for binary panel probit models, *Computational Statistics & Data Analysis* 55 (2011) 261–279. doi:10.1016/j.csda.2010.04.016.

S. Frühwirth-Schnatter, Model-based clustering of time series-a review from a bayesian perspective, 2011.

D. McParland, I. C. Gormley, Model based clustering for mixed data: clustmd, *Advances in Data Analysis and Classification* 10 (2016) 155–169. doi:10.1007/s11634-016-0238-x.

B. Grün, Model-based clustering, in: *Handbook of mixture analysis*, Chapman and Hall/CRC, 2019, pp. 157–192.

P. J. Lenk, W. S. DeSarbo, Bayesian inference for finite mixtures of generalized linear models with random effects, *Psychometrika* 65 (2000) 93–119. doi:10.1007/BF02294188.

S. Kim, M. G. Tadesse, M. Vannucci, Variable selection in clustering via Dirichlet process mixture models, *Biometrika* 93 (2006) 877–893. doi:10.1093/biomet/93.4.877.

H. Z. Yerebakan, B. Rajwa, M. Dundar, The infinite mixture of infinite gaussian mixtures, in: *Advances in Neural Information Processing Systems*, volume 27, Curran Associates, Inc., 2014.

M. Kyung, Dirichlet process mixtures of linear mixed regressions, *Communications for Statistical Applications and Methods* 22 (2015) 625–637. doi:10.5351/CSAM.2015.22.6.625.

H. Ishwaran, L. F. James, Gibbs sampling methods for stick-breaking priors, *Journal of the American Statistical Association* 96 (2001) 161–173. doi:10.1198/016214501750332758.

T. Park, J.-H. Jeong, J. W. Lee, Bayesian nonparametric inference on quantile residual life function: Application to breast cancer data, *Statistics in Medicine* 31 (2012) 1972–1985. doi:10.1002/sim.5353.

H. Park, T. Park, Y.-S. Lee, Partially collapsed Gibbs sampling for latent Dirichlet allocation, *Expert Systems with Applications* 131 (2019) 208–218. doi:10.1016/j.eswa.2019.04.028.

A. Gelman, J. B. Carlin, H. S. Stern, D. B. Dunson, A. Vehtari, D. B. Rubin, *Bayesian Data Analysis*, CRC Press etc., 2015.

D. A. van Dyk, T. Park, Partially collapsed Gibbs samplers: Theory and methods, *Journal of the American Statistical Association* 103 (2008) 790–796. doi:10.1198/016214508000000409.

T. Park, D. A. van Dyk, Partially collapsed Gibbs samplers: Illustrations and applications, *Journal of Computational and Graphical Statistics* 18 (2009) 283–305. doi:10.1198/jcgs.2009.08108.

S. Vines, W. Gilks, P. Wild, Fitting bayesian multiple random effects models, *Statistics and Computing* 6 (1996) 337–346. doi:10.1007/BF00143554.

X.-L. Meng, D. van Dyk, Fast em-type implementations for mixed effects models, *Journal of the Royal Statistical Society: Series B (Statistical Methodology)* 60 (1998) 559–578. doi:10.1111/1467-9868.00140.

D. A. van Dyk, Fitting mixed-effects models using efficient em-type algorithms, *Journal of Computational and Graphical Statistics* 9 (2000) 78–98. doi:10.1080/10618600.2000.10474867.

Y. Kim, Y.-K. Choi, S. Emery, Logistic regression with multiple random effects: A simulation study of estimation methods and statistical packages, *The American Statistician* 67 (2013) 171–182. doi:10.1080/00031305.2013.817357.

T. Park, S. Min, Partially collapsed gibbs sampling for linear mixed-effects models, *Communications in Statistics-Simulation and Computation* 45 (2016) 165–180.

S. Jeong, T. Park, D. A. van Dyk, Bayesian model selection in additive partial linear models via locally

adaptive splines, *Journal of Computational and Graphical Statistics* 31 (2022) 324–336.

H. Wallach, S. Jensen, L. Dicker, K. Heller, An alternative prior process for nonparametric Bayesian clustering, in: *Proceedings of the Thirteenth International Conference on Artificial Intelligence and Statistics*, 2010.

J. G. Scott, J. O. Berger, Bayes and empirical-bayes multiplicity adjustment in the variable-selection problem, *The Annals of Statistics* 38 (2010) 2587–2619. doi:10.1214/10-AOS792.

F. Liang, R. Paulo, G. Molina, M. A. Clyde, J. O. Berger, Mixtures of  $g$  priors for bayesian variable selection, *Journal of the American Statistical Association* 103 (2008) 410–423. doi:10.1198/016214507000001337.

A. Zellner, On assessing prior distributions and Bayesian regression analysis with g-prior distributions, *Bayesian Inference and Decision Techniques: Essays in Honor of Bruno De Finetti* 6 (1986) 233–243.

P. Papastamoulis, G. Iliopoulos, An artificial allocations based solution to the label switching problem in Bayesian analysis of mixtures of distributions, *Journal of Computational and Graphical Statistics* 19 (2010) 313–331. doi:10.1198/jcgs.2010.09008.

A. Gelman, D. B. Rubin, Inference from iterative simulation using multiple sequences, *Statistical Science* 7 (1992) 457–472. doi:10.1214/ss/1177011136.

[dataset] R. T. Riphahn, A. Wambach, A. Million, Incentive effects in the demand for health care: a bivariate panel count data estimation, *Journal of Applied Econometrics* 18 (2003) 387–405. doi:10.1002/jae.680.